


# Broadband asymmetric transmission for linearly and circularly polarization based on sand-clock structured metamaterial

Tao Fu(傅涛), Xing-Xing Liu(刘兴兴), Guo-Hua Wen(文国华), Tang-You Sun(孙堂友), Gong-Li Xiao(肖功利), and Hai-Ou Li(李海鸥)

**Citation:**Chin. Phys. B, 2021, 30 (**1**): 014201. DOI: 10.1088/1674-1056/abb662
Journal homepage: http://cpb.iphy.ac.cn; http://iopscience.iop.org/cpb

**What follows is a list of articles you may be interested in**

---

## Active metasurfaces for manipulatable terahertz technology

Jing-Yuan Wu(吴静远), Xiao-Feng Xu(徐晓峰), Lian-Fu Wei(韦联福)
Chin. Phys. B, 2020, 29 (**9**): 094202. DOI: 10.1088/1674-1056/aba613

## Hyperbolic metamaterials for high-efficiency generation of circularly polarized Airy beams

Lin Chen(陈林), Huihui Li(李会会), Weiming Hao(郝玮鸣), Xiang Yin(殷祥), Jian Wang(王健)
Chin. Phys. B, 2020, 29 (**8**): 084210. DOI: 10.1088/1674-1056/ab96a1

## Dynamically adjustable asymmetric transmission and polarization conversion for linearly polarized terahertz wave

Tong Li(李彤), Fang-Rong Hu(胡放荣), Yi-Xian Qian(钱义先), Jing Xiao(肖靖), Long-Hui Zhang(张隆辉), Wen-Tao Zhang(张文涛), Jia-Guang Han(韩家广)
Chin. Phys. B, 2020, 29 (**2**): 024203. DOI: 10.1088/1674-1056/ab5ef8

## Optical properties of a three-dimensional chiral metamaterial

Juan-Juan Guo(郭娟娟), Mao-Sheng Wang(汪茂胜), Wan-Xia Huang(黄万霞)
Chin. Phys. B, 2017, 26 (**12**): 124211. DOI: 10.1088/1674-1056/26/12/124211

## A planar chiral nanostructure with asymmetric transmission of linearly polarized wave and huge optical activity in near-infrared band

Liu Dao-Ya, Luo Xiao-Yang, Liu Jin-Jing, Dong Jian-Feng
Chin. Phys. B, 2013, 22 (**12**): 124202. DOI: 10.1088/1674-1056/22/12/124202

---

# Broadband asymmetric transmission for linearly and circularly polarization based on sand-clock structured metamaterial*

Tao Fu(傅涛)[1,†], Xing-Xing Liu(刘兴兴)[1], Guo-Hua Wen(文国华)[2], Tang-You Sun(孙堂友)[1], Gong-Li Xiao(肖功利)[1], and Hai-Ou Li(李海鸥)[1]

[1] *Guangxi Key Laboratory of Precision Navigation Technology and Application, Guilin University of Electronic Technology (GUET), Guilin* 541004, *China*
[2] *Department of Mechanical and Biomedical Engineering, City University of Hong Kong,* 83 *Tat Chee Ave, Kowloon, Hong Kong SAR, China*

(Received 8 June 2020; revised manuscript received 2 August 2020; accepted manuscript online 9 September 2020)

We proposed a sandwich structure to realize broadband asymmetric transmission (AT) for both linearly and circularly polarized waves in the near infrared spectral region. The structure composes of a silica substrate and two sand-clock-like gold layers on the opposite sides of the substrate. Due to the surface plasmons of gold, the structure shows that the AT parameters of linearly and circularly polarized waves can reach 0.436 and 0.403, respectively. Meanwhile, a broadband property is presented for the AT parameter is over 0.3 between 320 THz and 340 THz. The structure realizes a diode-like AT for linearly wave in forward and circularly wave in backward, respectively. The magnetic dipoles excited by current in the two gold layers contribute to the broadband AT. The current density in top and bottom metallic layers illustrates the mechanism of the polarization conversion for broadband AT in detail.

**Keywords:** asymmetric transmission, metasurface, polarization conversion, trerahertz, broadband, electromagnetic wave, near-infrared

**PACS:** 42.25.Bs, 42.25.Ja, 42.79.Ci, 81.05.Xj **DOI:** 10.1088/1674-1056/abb662

## 1. Introduction

Metasurfaces are artificial subwavelength structures that can manipulate the propagation of waves in various exotic electromagnetic devices.[1–8] Since Pendry *et al.*[9] pointed out that noble material can support surface plasmons (SPs) in visible light range, plasmonic metamaterials have attracted much attention of the world. Asymmetric transmission (AT) has been a hotspot of the metamaterial fields since Fedotov *et al.*[10] first reported a previously unknown phenomenon in a planar chiral structure patterned for circularly polarized waves.[11–13] The theory of advanced Jones calculus for analyzing AT metamaterials was proposed to resolve the different classification of asymmetric structures.[14,15] Afterwards, many planar metamaterial structures have been discussed from microwave to visible light.[11,12,15,16] Mehmet *et al.*[17] realized diode-like AT of linearly polarized waves using magnetoelectric coupling and electromagnetic wave tunneling. Many researchers were interested in the circularly polarized waves.[16,18] Furthermore, to realize the AT for linearly polarized waves, the mirror symmetry of the planar structure along the transmission direction must be broken down.[17–20] Recently, a kind of chiral structures for either linearly or circularly polarized waves were proposed to realize dual-band in microwave frequency or broadband AT in the near-infrared, visible band for one polarized wave.[21–26] Even tunable AT using new materials, such as graphene,[27] $VO_2$,[28] omega-shaped metamaterial,[29] and Dirac semimetals,[30] was presented in the last several years.[31–33] However, few works reported a broadband diode like AT for linearly and circularly polarized waves in terahertz regions.

In this paper, a new two-dimensional sand-clock like chiral structure is proposed to realize broad band AT properties for both linearly and circularly in near infrared region. The structure consists of two asymmetric sand-clock like gold films attached to the two opposite sides of a silica substrate. Based on the SPs effect of gold in near infrared region, the $y$-polarized wave is transmitted well and $x$-polarized wave is blocked in the backward ($-z$) direction. The total transmission of the right circularly polarized wave (RCP) is forbidden while the left circularly polarized wave (LCP) is relatively transparent in the forward ($+z$) direction. We will illustrate the relations between AT properties and the optical activities of both linearly and circularly polarized light in detail.

## 2. Theoretical analysis of the broadband asymmetric transmission

We study an incident wave $E_i(r,t) = (E_x^i, E_y^i)^{\mathrm{T}} \mathrm{e}^{\mathrm{i}(kz-\omega t)}$ with angular frequency $\omega$, wave vector $k$, and complex amplitudes $E_x^i$ and $E_y^i$, propagating through anisotropic structures in the $+z$ direction. Usually, the linearly polarized transmis-

*Project supported by the National Natural Science Foundation of China (Grant Nos. 11965009, 61874036, 61805053, and 61764001), the Natural Science Foundation of Guangxi Zhuang Autonomous Region, China (Grant Nos. 2018JJA170010 and 2018GXNSFAA281193), and the Innovation Project of GUET Graduate Education (Grant No. 2020YCXS019).

†Corresponding author. E-mail: ft85@guet.edu.cn

© 2021 Chinese Physical Society and IOP Publishing Ltd 

sion matrix $\hat{T}$ is employed to connect the generalized complex amplitudes of the transmitted wave with the incident fields as follows:[34]

$$\begin{pmatrix} E_x^{\rm t} \\ E_y^{\rm t} \end{pmatrix} = \hat{T} \begin{pmatrix} E_x^{\rm i} \\ E_y^{\rm i} \end{pmatrix} = \begin{pmatrix} T_{xx}^{\rm f} & T_{xy}^{\rm f} \\ T_{yx}^{\rm f} & T_{yy}^{\rm f} \end{pmatrix} \begin{pmatrix} E_x^{\rm i} \\ E_y^{\rm i} \end{pmatrix} = \hat{T}_{\rm lin}^{\rm f} \begin{pmatrix} E_x^{\rm i} \\ E_y^{\rm i} \end{pmatrix}. \quad (1)$$

The superscript f indicates the propagation direction of the incident wave is forward. $E_x^{\rm t}$ and $E_y^{\rm t}$ denote the $x$ and $y$ components of the transmitted electric field, respectively. For a medium made of reciprocal system, the transmission matrix $T_{\rm lin}^{\rm b}$ for the case in the $-z$ direction can be revised as[14]

$$T_{\rm lin}^{\rm b} = \begin{pmatrix} T_{xx}^{\rm b} & T_{xy}^{\rm b} \\ T_{yx}^{\rm b} & T_{yy}^{\rm b} \end{pmatrix} = \begin{pmatrix} T_{xx}^{\rm f} & -T_{yx}^{\rm f} \\ -T_{xy}^{\rm f} & T_{yy}^{\rm f} \end{pmatrix}. \quad (2)$$

The difference in the transmittance (transmitted intensity divided by the incident intensity) for waves propagating along two opposite directions (in our case the forward (positive) and backward (negative) $-z$ direction) can be defined as the following expression:

$$\begin{aligned} \Delta_{\rm lin}^{(x)} &= \left|T_{xx}^{\rm f}\right|^2 + \left|T_{yx}^{\rm f}\right|^2 - \left|T_{xx}^{\rm b}\right|^2 - \left|T_{yx}^{\rm b}\right|^2 \\ &= \left|T_{yx}^{\rm f}\right|^2 - \left|T_{xy}^{\rm f}\right|^2 = -\Delta_{\rm lin}^{(y)}. \end{aligned} \quad (3)$$

Consequently, the transmission matrix of circularly polarized can be expressed as the four elements of linearly polarized transmission matrix:[14]

$$T_{\rm cir}^{\rm f} = \begin{pmatrix} T_{++}^{\rm f} & T_{+-}^{\rm f} \\ T_{-+}^{\rm f} & T_{--}^{\rm f} \end{pmatrix} = \frac{1}{2} \begin{pmatrix} (T_{xx}^{\rm f} + T_{yy}^{\rm f}) + {\rm i}(T_{xy}^{\rm f} - T_{yx}^{\rm f}) & (T_{xx}^{\rm f} - T_{yy}^{\rm f}) - {\rm i}(T_{xy}^{\rm f} + T_{yx}^{\rm f}) \\ (T_{xx}^{\rm f} - T_{yy}^{\rm f}) + {\rm i}(T_{xy}^{\rm f} + T_{yx}^{\rm f}) & (T_{xx}^{\rm f} + T_{yy}^{\rm f}) - {\rm i}(T_{xy}^{\rm f} - T_{yx}^{\rm f}) \end{pmatrix}. \quad (4)$$

In which subscripts '+' and '−' denote right (RCP) and left (LCP) circular polarizations, respectively. For circularly polarized wave, the AT effect can be expressed as

$$\Delta_{\rm circ}^{(+)} = \left|T_{-+}^{\rm f}\right|^2 - \left|T_{+-}^{\rm f}\right|^2 = -\Delta_{\rm circ}^{(-)}. \quad (5)$$

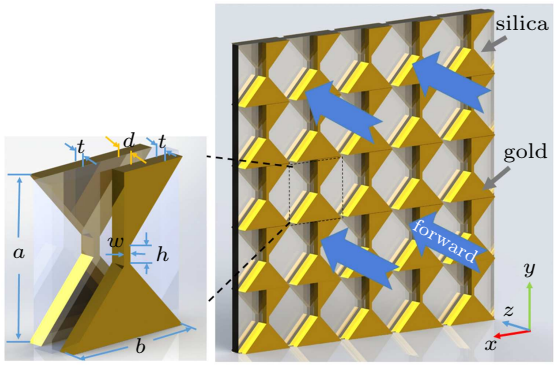



**Fig. 1.** Schematic diagram of the sand-clock AT structure.

Figure 1 shows the schematic diagram of a unit cell and the sand-clock structure metamaterial employed in this study. The whole structure consisting of three layers, a non-symmetrical metallic bottom layer, the dielectric substrate layer and symmetrical metallic top layer, endows symmetric breaking along the $z$ direction of propagation. The material of dielectric substrate is silica with relative permittivity ($\varepsilon = 2.1$), thickness $d = 60$ nm, and dimension of 400 nm× 400 nm. Periodic boundary conditions are applied to the unit cell along both $x$ and $y$ directions. An incident plane wave propagating along the $+z$ direction is considered as the forward direction. Numerical simulations were performed with commercial three-dimensional full-wave solver (CST Microwave Studio, Computer Simulation Technology, Germany) based on the finite element method. After parametric optimization, the parameters of the unit cell are as follows: $a = 400$ nm, $b = 350$ nm, $h = 45$ nm, $w = 20$ nm. The gold films (thickness $t = 40$ nm) is dealt with the Drude model ($\omega_{\rm p} = 2\pi\times2.175\times10^{15}$ (rad/s), $\omega_{\rm c} = 2\pi\times6.5\times10^{12}$ (1/s)).

## 3. Results and discussion

According to the theory of AT, we simulated the transmission coefficients of the model in Fig. 1. After parameters optimized, figure 2 shows the four elements of transmission matrix both in backward ($-z$) and forward ($+z$) directions, respectively.

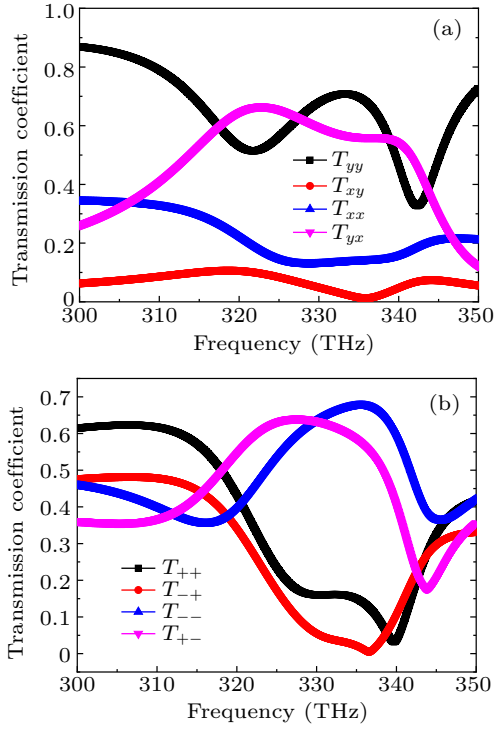



**Fig. 2.** Transmission coefficients (absolute value) of (a) linearly polarized and (b) circularly polarized waves in the forward direction.

For the cross-polarized transmission in Fig. 2(a), $T_{yx}$ can reach more than 0.5 from 315 THz to 340 THz and arrive at the maximum point 0.67 at 322.8 THz. While the magnitude of $T_{xy}$ remains lower than 0.1 almost in the whole range. The obvious difference between $T_{yx}$ and $T_{xy}$ renders a strong asymmetric transmission effect. The transmission coefficient $T_{xx}$ and $T_{yy}$ are not equal to each other for the asymmetric gold layers on the opposite side of the substrate.[14] The transmission coefficients of the circularly polarized wave in Fig. 2(b) give a high $T_{-+}$ contrast to lower $T_{+-}$ from 320 THz to 340 THz. The clear difference between $T_{-+}$ and $T_{+-}$ represents an evident AT effect for circularly wave. Meanwhile, $T_{++}$ is entirely different from $T_{--}$ from 320 THz to 340 THz. $T_{++}$ almost reduces from 0.62 to 0 between 310 THz and 340 THz. On the contrary, $T_{--}$ increases from 0.5 (323 THz) to 0.677 (336 THz) and descents to 0.5 till 342 THz.

According to Eqs. (3) and (5), the AT parameters for both linear and circular polarizations are depicted in Fig. 3. From Fig. 3(a), the asymmetric transmission parameters of linearly polarized waves attain to the maximum of $\pm 0.463$ at the frequency of 321.9 THz. The AT parameter exceeds 0.3 from 315 THz to 340 THz, which realizes broadband AT. Furthermore, the AT parameters of the circularly polarized waves are shown in Fig. 3(b). The parameters of $\Delta_{\mathrm{circ}}^{(+)}$ and $\Delta_{\mathrm{circ}}^{(-)}$ exhibiting opposite sign can reach a maximum of $\pm 0.403$ at frequency of 328.5 THz. All these properties of the sand-clock structure illustrate that it can support the AT both in linearly and circularly wave in a broad band.

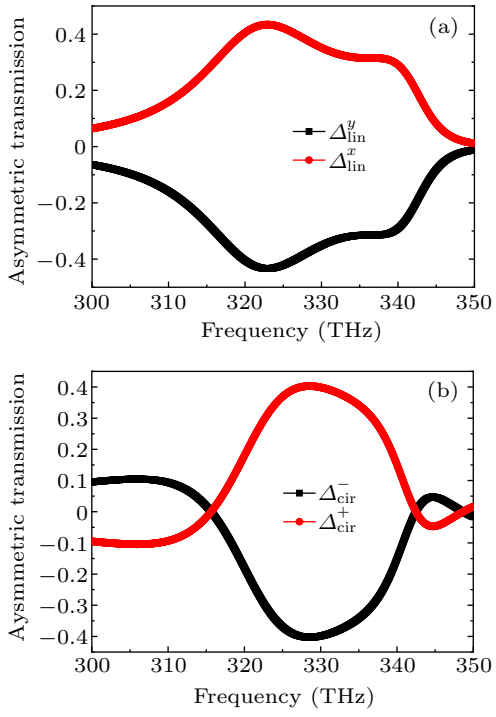



**Fig. 3.** The asymmetric transmissions of (a) linearly polarized and (b) circularly polarized waves.

Figure 4 shows the total transmissions ($|\boldsymbol{T}_x^{\mathrm{f}}| = |T_{xx}^{\mathrm{f}}|^2 + |T_{yx}^{\mathrm{f}}|^2$, $|\boldsymbol{T}_y^{\mathrm{f}}| = (|T_{yy}^{\mathrm{f}}|^2 + |T_{xy}^{\mathrm{f}}|^2)^{1/2}$, $|\boldsymbol{T}_+^{\mathrm{f}}| = (|T_{++}^{\mathrm{f}}|^2 + |T_{-+}^{\mathrm{f}}|^2)^{1/2}$, and $|\boldsymbol{T}_-^{\mathrm{f}}| = (|T_{--}^{\mathrm{f}}|^2 + |T_{+-}^{\mathrm{f}}|^2)^{1/2}$) of all polarizations in the $+z$ ($-z$) direction.[34] For linearly polarized wave in Fig. 4(a), the total transmission of the $y$-polarized wave in the backward ($-z$) direction reaches the maximum of 0.83 in the simulation, however, the total transmission of the $x$-polarized wave is nearly zero from 320 THz to 345 THz. These results indicate that the $y$-polarized wave transmits well and the $x$-polarized waves are forbidden in the backward direction.[23] This effect is similar to an electronic diode that can allow the electric current to flow through it in one direction while blocking the electric current in the opposite direction.[10,12] While the $x$- and $y$-polarized waves have no significant 'zero' *versus* 'large' transmission difference along the opposite direction ($+z$) in the whole region.

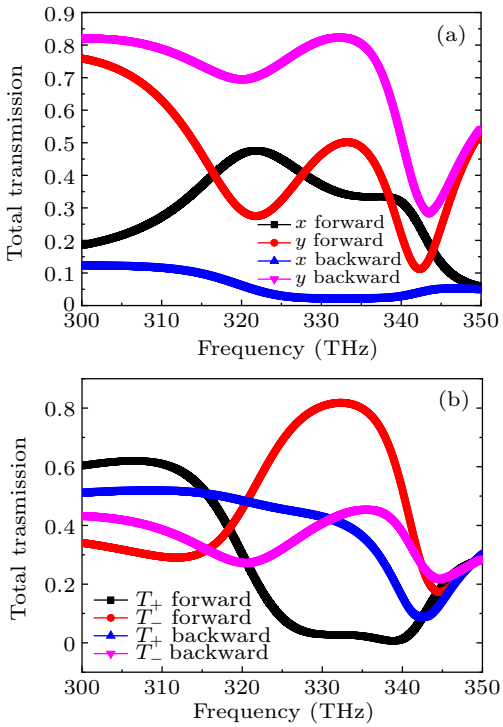



**Fig. 4.** Total transmission of (a) $x$ and $y$ linearly polarized waves, and (b) left and right circularly polarized waves in forward and backward directions.

Observing the total transmission results of circularly polarized wave in Fig. 4(b), the total transmission of the RCP is lower than that of the LCP from 320 THz to 340 THz in the forward direction. The total transmission of the LCP can reach to the maximum 0.82 while that of the RCP is close to zero in the forward direction. Then, the structure can become a polarization isolator for the RCP wave. The large difference between forward and backward comes from the AT index in Fig. 3. Therefore, the structure can be designed as an AT diode for the backward $y$ linear wave and the forward LCP circular wave respectively.

## 4. Origin of the asymmetric transmission

The physical origin of this broadband AT effects, the current density of the hybridized plasmon mode excited by lin-

early and circularly polarized waves at different frequencies is demonstrated in the following Fig. 5. The black arrows represent the current density direction in the metallic layers. An electromagnetic field causes the excitation of an electric dipole with parallel currents and a magnetic dipole with anti-parallel currents. The interaction between a magnetic dipole and an electric dipole will result in the strong coupling and high transmission.[35]

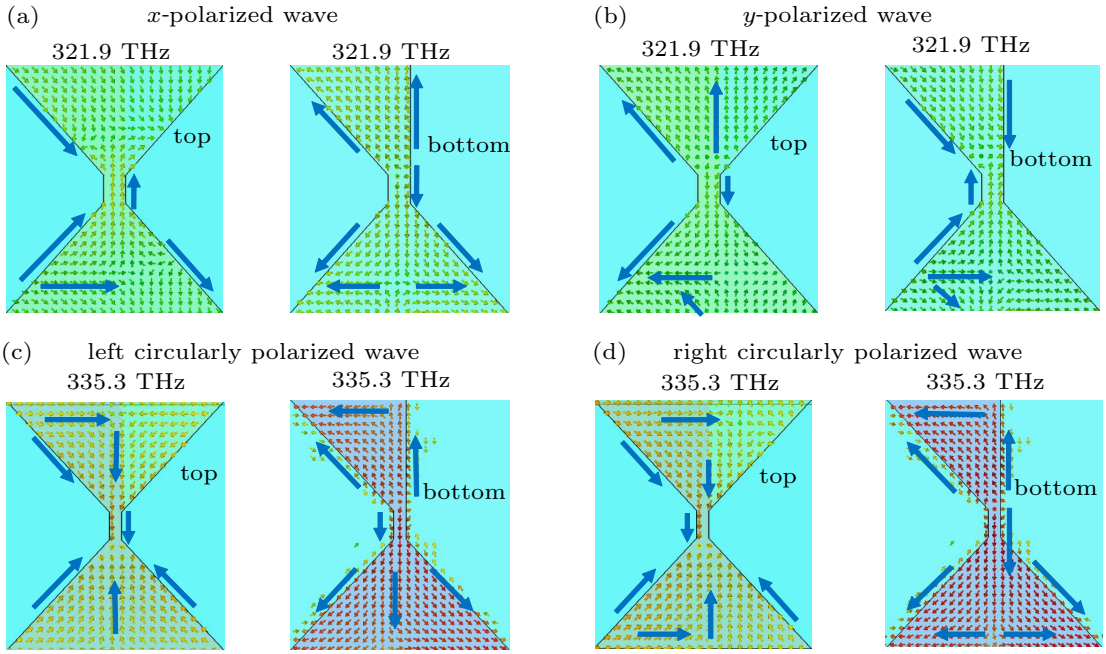



**Fig. 5.** Current densities of linearly and circularly polarized waves in metallic layers for (a), (b) 321.9 THz and (c), (d) 335.3 THz, respectively.

To further research the mechanism of the broad band AT, we analyzed the current densities distribution when the plane wave propagates through the chiral sand-clock structure at the resonant frequency 321.9 THz and 335.3 THz in Fig. 5, respectively. From Figs. 5(a)–5(d), when an arbitrary polarized wave is incident to the structure, the magnetic dipoles are excited by the current density aligned anti-parallel between the top and bottom metallic layers.[13,36] The magnetic dipoles lead the whole broadband AT from 300 THz to 340 THz. From the current density on the neck part of the sand-clock structure at 321.9 THz, it is easily found that the couple intensity of the *y* direction contributes stronger than that of the *x* direction for both polarized waves, which results in higher transmission for backward *y*-polarized in Fig. 4(a). In Figs. 5(c) and 5(d), the current directions of left-polarized and right-polarized waves are consistent with each other at 335.3 THz. This indicates the left-polarized waves coupling with the current very well can be transmitted through the structure while the right-polarized waves are reflected in the backward direction as shown in Fig. 2(b).

## 5. Conclusion and perspectives

In this work, we designed a sandwich structure with two gold layers on silica substrate to realize AT both for the linear and circular polarization in the region of the near infrared region. The AT parameters exhibited the structure can support broad band AT both for linear and circular polarization from 315 THz to 340 THz. The total transmission properties of the linearly and circularly polarized waves showed the diode like AT for linear polarization which can transmit *y*-polarized wave and block *x*-polarized wave in the backward direction. Furthermore, the RCP was forbidden, and the LCP was relatively transparent from 320 THz to 340 THz in the forward direction. In addition, we demonstrated the current density distribution of the two polarized waves at different frequencies to present the physical mechanism of AT. The structure may find potential applications in terahertz devices, such as terahertz isolators, polarizer, and so on.

## References

[1] Patrice G and Federico C 2015 *Rep. Prog. Phys.* **78** 024401
[2] Deng Z L, Zhang S and Wang G P 2016 *Nanoscale* **8** 1588
[3] Chen H T, Taylor A J and Yu N F 2016 *Rep. Prog. Phys.* **79** 076401
[4] Deng Z L, Cao Y, Li X and Wang G P 2018 *Photon Res.* **6** 443
[5] Yu N F and Capasso F 2014 *Nat. Mater.* **13** 139
[6] Deng Z L and Li G X 2017 *Mater. Today Phys.* **3** 16
[7] Wang Z J, Yao K, Chen M, Chen H S and Liu Y M 2016 *Phys. Rev. Lett.* **117** 157401
[8] Deng Z L, Deng J H, Zhuang X, Wang S, Li K F, Wang Y, Chi Y H, Ye X, Xu J, Wang G P, Zhao R K, Wang X L, Cao Y Y, Cheng X, Li G X and Li X P 2018 *Nano Lett.* **18** 2885
[9] Pendry J B, Holden A J, Stewart W J and Youngs I 1996 *Phys. Rev. Lett.* **76** 4773
[10] Fedotov V A, Mladyonov P L, Prosvirnin S L, Rogacheva A V, Chen Y and Zheludev N I 2006 *Phys. Rev. Lett.* **97** 167401

[11] ingh R, Plum E, Menzel C, Rockstuhl C, Azad A K, Cheville R A, Lederer F, Zhang W and Zheludev N I 2009 *Phys. Rev. B* **80** 153104
[12] Kenanakis G, Xomalis A, Selimis A, Vamvakaki M, Farsari M, Kafesaki M, Soukoulis C M and Economou E N 2015 *ACS Photon.* **2** 287
[13] Shang X J, Zhai X, Wang L L, He M D, Li Q, Luo X and Duan H G 2017 *Appl. Phys. Express* **10** 052602
[14] Menzel C, Rockstuhl C and Lederer F 2010 *Phys. Rev. A* **82** 053811
[15] Menzel C, Helgert C, Rockstuhl C, Kley E B, Tünnermann A, Pertsch T and Lederer F 2010 *Phys. Rev. Lett.* **104** 253902
[16] Pfeiffer C, Zhang C, Ray V, Guo L J and Grbic A 2014 *Phys. Rev. Lett.* **113** 023902
[17] Mutlu M, Akosman A E, Serebryannikov A E and Ozbay E 2012 *Phys. Rev. Lett.* **108** 213905
[18] Huang C, Feng Y J, Zhao J, Wang Z B and Jiang T 2012 *Phys. Rev. B* **85** 195131
[19] Liu D Y, Luo X Y, Liu J J and Don J F 2013 *Chin. Phys. B* **22** 124202
[20] Shi J H, Ma H F, Guan C Y, Wang Z P and Cui T J 2014 *Phys. Rev. B* **89** 165128
[21] Tang D F, Wang C, Pan W K, Li M H and Dong J F 2017 *Opt. Express* **25** 11329
[22] Xu K K, Xiao Z Y and Tang J Y 2016 *Opt. Quantum Electron.* **48** 381
[23] Tang B, Li Z Y, Liu Z Z, Callewaert F and Aydin K 2016 *Sci. Rep.* **6** 39166
[24] Liu D J, Xiao Z Y, Ma X L, Xu K K, Tang J Y and Wang Z H 2016 *Wave Motion* **66** 1
[25] Liu D J, Xiao Z Y, Ma X L and Wang Z H 2015 *Opt. Commun.* **354** 272
[26] Cheng Y Z, Gong R Z and Wu L 2016 *Plasmonics* **12** 1113
[27] Shi C Y Y, He X Y, Peng J, Xiao G N, Feng Liu, Lin F T and Zhang H 2019 *Opt. Laser Technol.* **114** 28
[28] Liu M, Xu Q, Chen X Y, Plum E, Li H, Zhang X Q, Zhang C H, Zou C W, Han J G and Zhang W L 2019 *Sci. Rep.* **9** 4097
[29] Wang Y H, Jin R C, Li J, Li J Q and Dong Z G 2018 *Opt. Express* **26** 3508
[30] Dai L L, Zhang Y P, O'Hara J F and Zhang H Y 2019 *Opt. Express* **27** 35784
[31] Li T, Hu F R, Qian Y X, Xiao J, Zhang L H, Zhang W T and Han J G 2020 *Chin. Phys. B* **29** 024203
[32] Jiang H, Zhao W Y and Jiang Y Y 2017 *Opt. Express* **25** 19732
[33] Li Y, Shen C, Xie Y B, Li J F, Wang W Q, Cummer S A and Jing Y 2017 *Phys. Rev. Lett.* **119** 035501
[34] Liu D J, Xiao Z Y, Ma X L, Ma Q W, Xu X X and Wang Z H 2015 *Opt. Commun.* **338** 359
[35] Liu N, Guo H C, Fu L W, Kaiser S, Schweizer H and Giessen H 2007 *Nat. Mater.* **7** 31
[36] Liu D J, Xiao Z Y, Ma X L and Wang Z H 2015 *Appl. Phys. Express* **8** 052001